Understanding and exploiting competing segregation mechanisms in horizontally rotated granular media

2016 New J. Phys. 18 023013

(http://iopscience.iop.org/1367-2630/18/2/023013)

New Journal of Physics
The open access journal at the forefront of physics

Deutsche Physikalische Gesellschaft DPG
IOP Institute of Physics

Published in partnership with: Deutsche Physikalische Gesellschaft and the Institute of Physics

OPEN ACCESS

RECEIVED
23 October 2015

REVISED
17 December 2015

ACCEPTED FOR PUBLICATION
21 December 2015

PUBLISHED
29 January 2016

PAPER

Understanding and exploiting competing segregation mechanisms in horizontally rotated granular media

C R K Windows-Yule[1,2], B J Scheper[1], A J van der Horn[1], N Hainsworth[2], J Saunders[2], D J Parker[2] and A R Thornton[1]

[1] Multi-Scale Mechanics, Dept. of Mechanical Engineering, MESA+, University of Twente, P.O. Box 217, 7500 AE Enschede, The Netherlands
[2] School of Physics and Astronomy, University of Birmingham, B15 2TT, UK

E-mail: windowsyule@gmail.com

Keywords: segregation, particulate flow, granular flow, mixing, rotating drum

Abstract

The axial segregation of granular and particulate media is a well-known but little-understood phenomenon with direct relevance to various natural and industrial processes. Over the past decades, many attempts have been made to understand this phenomenon, resulting in a significant number of proposed mechanisms, none of which can provide a full and universally applicable explanation. In this paper, we show that several mechanisms can be simultaneously active within a single system, and that by considering all relevant mechanisms, it is possible to understand and explain a system's segregative behaviours over a wider range of parameter space than is possible by considering any one, single process. We explore the interrelation and competition between the individual mechanisms present within a given system and demonstrate that by understanding these interactions, we can predict and even, through carefully designed systems, *control* their behaviour. In particular, we demonstrate that it is possible to *deliberately direct* segregation, allowing an arbitrary number of pre-determined segregation patterns to be induced in a system. We also illustrate a manner in which the competition between two opposing segregation mechanisms may be exploited in order to enhance the mixing of two dissimilar species of particle—a much sought after ability.

1. Introduction

Granular media are, after water, the second most manipulated substances on Earth [1], playing essential rôles in multitudinous industrial and natural processes [2–4]. As such, an understanding of these materials and their flow behaviours is imperative. One of the most frequently used apparatus with which to study granular materials is the horizontally rotating drum [5–8]. The popularity of the rotating drum geometry stems largely from two factors: firstly, due to its relative simplicity, it provides an easily-studied canonical system in which the fundamental behaviours of particulate flows may be investigated [9–11]. Secondly, this geometry is of direct relevance to a large number of important industrial processes [12–17].

One phenomenon which attracts considerable attention from both a scientific and industrial [18–21] standpoint is that of *segregation* [22], whereby a mixture of particles whose constituents differ in their geometry (e.g. size or shape) [23, 24] or material properties (e.g. density, elastic or frictional properties) [25, 26] may spontaneously separate into its individual components. An understanding of the manner in which materials segregate or mix is vital in a variety of processes. For instance, in the pharmaceutical industry [27–29], the unwanted separation of excipient and active ingredient may render certain batches of medicine entirely ineffective, and others highly dangerous. Conversely, in other situations the separation of individual components from a mixture is highly desirable; consider for example the extraction of valuable materials from electronic waste [30, 31]–a matter of significant financial [32] and environmental [33] importance on a global scale.

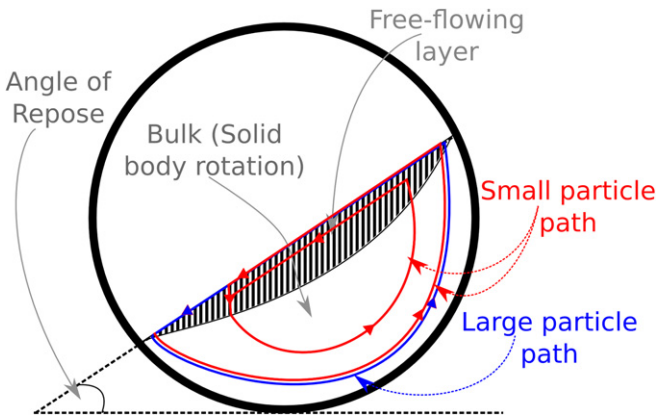

Figure 1. Simple schematic demonstrating the major features and and terminology associated with the rotating drum geometry. In the diagram, we see that the bed is divided broadly into a dense, solid-like 'bulk' wherein particles simply follow the trajectory of the rotating system in rigid body motion, and a more dilute, active upper layer. The majority of relative motion between particles occurs in this flowing layer, making it by definition the region in which segregative processes predominantly occur. Shown also in the diagram are illustrative examples representing typical paths followed by a single small and large particle. A large particle will typically follow the cascading layer from its start to its terminus, thus simply repeating the same—or a similar—path upon each drum rotation. For a small particle, meanwhile, there exists an increased probability that it will instead be 'sieved' downward through the free-flowing layer, thus accessing instead an inner streamline for the next rotation. As this process repeats, small particles on average will move toward more central regions, thus explaining the formation of a central core in rotating systems.

In a rotating drum, a particulate system may experience both *radial* segregation and *axial* segregation. In the former process, smaller [34, 35], and/or more dense [25, 36, 37] particles form a central core surrounded by a region of predominantly larger particles. More specifically, in the relatively loosely-packed flowing layer of a rotary system, smaller particles are more likely to be 'sieved' downwards [9] (see figure 1). Thus, these particles occupy the inner streamlines of the flow, resulting in the formation of a small particle core [34]. This process, illustrated schematically in figure 1, is relatively well known and widely accepted, and hence will not be discussed at length in this paper. The latter process of axial segregation or 'banding', meanwhile, remains poorly understood, with numerous different—and often incompatible—mechanisms proposed to explain its origins [38–40]. The lack of a general consensus as to the origins of axial segregation is, clearly, a hindrance to the development of a fuller understanding of this important phenomenon.

In this paper, we study the influence of system geometry on the axial segregation exhibited by a granular bed housed within a rotating drum. In doing so, we are able to test several contemporary theories regarding the axial segregation of such systems, with the following aims:

(i) To assess the *general validity* of three distinct mechanisms proposed in previous works.

(ii) To assess the *range of validity* of each mechanism with respect to several geometric properties.

(iii) To explore the interactions between differing mechanisms under various conditions and the circumstances under which each may become dominant or negligible.

(iv) To demonstrate methods through which the competition and cooperation between segregative mechanisms may be exploited in order to enhance and direct segregation or, conversely, to induce or improve mixing.

1.1. Previously proposed mechanisms for axial segregation

There exists a wealth of literature pertaining to the segregation of rotated particulate systems [41] and indeed the effects of system geometry on this segregation [38, 42–49]. Since a full discussion of these previous works would, in and of itself, result in a sizeable article, we focus here on those whose influence we see significant evidence of in our own data.

In their 1994 paper, Zik *et al* [50] suggested that axial segregation may occur due to the presence of spontaneous localised fluctuations in the angle of repose (see figure 1) of a granular assembly along the axial length of the rotating system in which it is housed. Specifically, it was proposed that more mobile particles would preferentially move down the axial gradients produced by these differences, thus exacerbating the effect, as the resultant excess of more mobile particles would further decrease the angle of repose. Thus, in a process analogous to spinodal decomposition [51], the system eventually achieves an axially segregated state. Moreover,

Zik *et al* also demonstrated that the requisite differences in angle of repose could be *deliberately induced* by modulating the tube diameter, producing a clearly defined axial banding even in previously non-segregative systems.

In 2011, Fan and Hill [52, 53] proposed a mechanism to describe axial segregation in chute flows. Their theory can perhaps be most easily understood as a kinetic-stress-driven analogue to the Gray-Thornton model of segregation [23, 54]. The model of Gray and Thornton states that segregation in the direction parallel to gravity can be explained by the fact that larger particles feel a greater lithostatic pressure per unit volume as compared to smaller particles, which are more likely at any point in time to be 'falling through' voids within the system [55] and hence experiencing no force from the bed below. This imbalance in the upward pressure provided to the differing particle species will naturally lead to a tendency for large particles to rise upwards through a system and smaller particles to sink downwards, as is indeed routinely observed in various granular flows [56–60].

Fan and Hill [52, 53] suggest that a similar process may explain segregation in the direction perpendicular to gravity—i.e. the axial direction. Specifically, they note that larger particles bear a greater proportion of the *contact stress* than they do the *kinetic stress*, with the inverse being true for smaller particles. Thus, while all particles are in essence pushed away from regions of higher fluctuation energy, $\tilde{E}$, the process is more efficient for smaller particles, which may more easily filter through small pores in the system through the process of 'squeeze expulsion' [55, 56]. This results in a net migration of small particles towards low-$\tilde{E}$ regions of the system, and hence a net flux of larger particles towards higher-$\tilde{E}$ regions. Note that this process occurs only for relatively dense systems, with sparser beds known to exhibit the exact inverse behaviour [61–64].

The kinetic stress model was later applied to the rotating drum geometry [65] where it was compared against results acquired from numerical simulations. However, in this paper, the theory was only applied to segregation in the *radial*—as opposed to axial—direction. Thus, one of the primary outcomes of this paper is the provision of evidence supporting the validity of the model of [52] in this geometry. Our work also represents the first time that the theory of Fan and Hill [52, 53] has been investigated in an *experimental* rotating system—an important test of its real-world applicability. Further discussion of the model of Fan and Hill and its presence in our systems may be found in section 3.3.

The 2015 paper of Gonzalez *et al* [66] demonstrated an additional manner in which system geometry may be utilised to induce and direct axial segregation in rotated systems. In this work, it was demonstrated that a system divided axially into a convex and a concave region would produce a rapid axial segregation, with large particles predominantly occupying convex regions and smaller particles preferentially inhabiting concave regions. However, two dissimilar regular polygons inscribed on a circle of the same diameter will, by definition, possess differing cross-sectional areas. As such, one must raise the question as to whether the results of [66] simply arise from the mechanism described by Zik *et al* [50] due to differences in the effective cylinder diameter. Later in this paper (section 3.4), we will demonstrate that the segregative processes proposed by Zik *et al* [50] and Gonzalez *et al* [66] are indeed distinct, and also establish the relative strength of the two mechanisms. It is additionally worth noting that there remains a second open question as to whether the observations of Gonzalez *et al* are generalisable to all convex-concave pairings, or only the single pairing used in the previous study. This issue will also be resolved in the current work (see section 3.1).

As mentioned above, there exists strong evidence of all three of the above-described mechanisms in our experimental system. In the following pages, we will assess the influence of various aspects of system geometry on each of these mechanisms, and the complex interrelations between them.

1.2. Outline and aims

Due to the broad scope of the subject matter discussed this paper is, for clarity, divided into a number of sections. We begin in section 2.1 by describing our experimental set-up and detailing the various manners in which the geometry of our system may be varied in order to alter the dynamics of the particulate system housed within. We then explain, in section 2.2, the manner in which data is acquired from our system using Positron Emission Particle Tracking (PEPT).

Our results and analysis section (section 3) is partitioned into several subsections. In section 3.1 we demonstrate that the segregation mechanism of Gonzalez *et al* [66], which for brevity we shall simply refer to throughout this paper as the 'CC' ('convex-concave') mechanism, can seemingly be generalised to any convex-concave pairing of shapes. In the following subsection (section 3.2) we show that the CC mechanism can be exploited in order to *deliberately induce and control* axial banding through the use of drums comprising multiple alternating convex and concave axial segments; we demonstrate that this ability may be used to produce an arbitrary number of complex segregation patterns. In section 3.3, we provide first experimental evidence of the kinetic-stress-induced segregation mechanism of Hill and Fan. We then conclude our results section with an exploration of the interactions between the segregation mechanisms of Zik *et al* , Fan and Hill and Gonzalez *et al* (section 3.4). We show that all three mechanisms are seemingly present in our system, with the relative strength

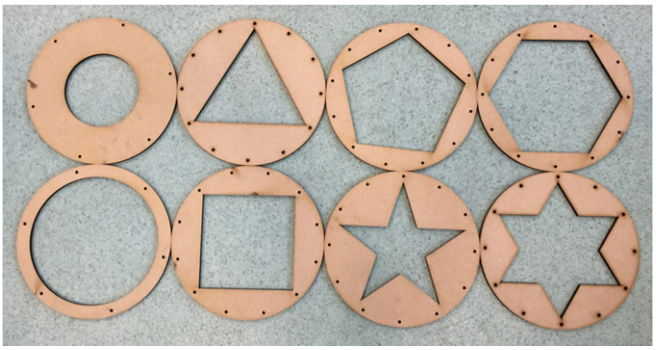

Figure 2. The various polygonal drum sections used in experiment. The geometries chosen correspond to the 4 simplest regular convex polygons and the 2 simplest regular concave polygons. With the exception of the smaller circular geometry, which possesses a diameter of 150 mm, all shapes share a common maximal diameter of 250 mm–i.e. all polygons are inscribed on the same circle.

of each varying considerably as the geometry of the system is altered. It is also demonstrated that the mixing of a multi-component granular assembly may be improved by constructing the containing system's geometry so as to *balance* opposing segregation mechanisms–an observation of potential significance in various practical applications.

Finally, in section 4, we summarise our results and present our major conclusions.

2. Experimental details

2.1. Experimental set-up

Our basic experimental set-up consists of a binary bed of 3 and 4 mm chrome steel particles housed within a drum which is rotated about its horizontal axis at a fixed rate of 25 rpm, producing a continuously avalanching layer of particles along the free surface of the bed [67, 68]. The drum is constructed from a series of individual, laser-cut sections (see figure 2), allowing systems of various length, $18 \leqslant L \leqslant 126$ mm, and internal geometry to be created and studied. With the exception of the smaller circular geometry, whose inclusion allows us to directly isolate and test the effects of differing segment area, all polygons explored are inscribed on the same 250 mm diameter circle. As the length and/or internal geometry of the system are varied, the number of particles within the system is adjusted such that a constant filling fraction, $F = 0.4$, and a constant 1:1 volume ratio of small to large particles are maintained. The filling fraction, F, refers to the volume of the granular bed as a whole, including both grain volume, V_g, and void space, divided by the total volume of the container, V_c. The constant filling fraction of $F = 0.4$ used in our experiments corresponds to an 'absolute' filling fraction $F_{\text{abs.}} = \frac{V_g}{V_c} = 0.24$. Throughout this manuscript, the larger and smaller species of particle may be referred to as species 'l' and species 's', respectively. This nomenclature not only aids brevity, but also allows the indices l, s to denote physical quantities pertaining only to a specific species.

The experimental system is placed between the detector heads of an ADAC *Forté* dual-headed gamma camera, allowing the internal dynamics of the system to be analysed using positron emission particle tracking (see section 2.2, below). Data are acquired from the system over a period $7200 \leqslant t_{\text{exp.}} \leqslant 14400$ s, corresponding to between 3000 and 6000 drum revolutions. Experiments using longer drums are conducted over greater durations to allow the tracer particle to fully explore the system, thus ensuring good statistics [69, 70] for PEPT measurements.

2.2. Data acquisition–positron emission particle tracking

Our system is analysed using positron emission particle tracking (PEPT) [71]. In order to perform PEPT, a single particle from the system is exposed to a high-energy proton beam from the Birmingham cyclotron. This acts to induce β^+ radioactivity within the particle material through the conversion of iron (^{56}Fe) atoms to radioactive cobalt-55 (^{55}Co) via the reaction ^{56}Fe $(p, 2n)$ ^{55}Co. This process leaves the particle physically identical to all others of its species, making PEPT an entirely non-invasive technique.

The positrons emitted by the cobalt isotopes will rapidly annihilate with electrons within the dense tracer medium, producing a pair of 511 keV γ-rays whose trajectories are separated by $180 \pm 0.5^\circ$. If both γ-photons are detected by the positron camera used to image the system, the linear path followed can be reconstructed algorithmically. Thus, by finding the intersection of a number of such reconstructed paths, it is possible to triangulate the spatial position of the tracer. For an adequately active particle, a large number of triangulation

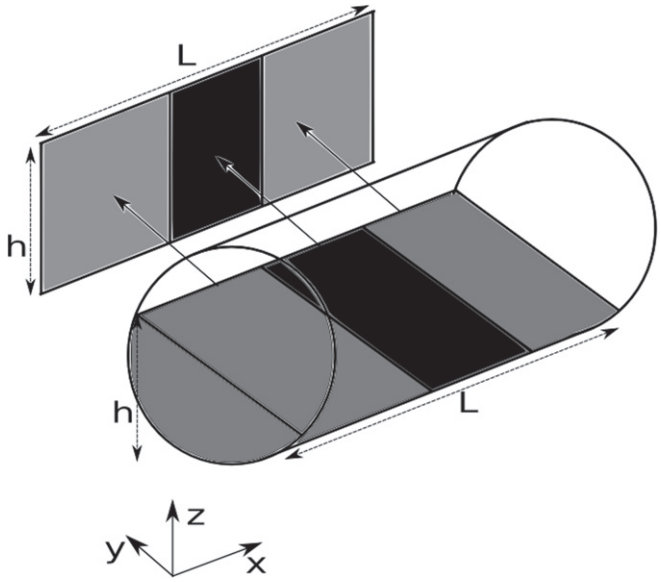

Figure 3. Visual representation (not to scale) of the correspondence between the two-dimensional depth-averaged 'projections' of the system provided throughout this manuscript and the three-dimensional system being imaged. In all cases, data are averaged through the horizontal *y*-direction as defined in this figure such that axial variations in the various fields presented may be clearly observed in the two-dimensional *x*-*z* plane.

events can be performed per second, allowing the motion of the tracer particle through the system to be recorded, in three dimensions, with sub-millimetre accuracy and temporal resolution of the order of milliseconds [69]. Due to the highly-penetrating γ-rays used, particles can be tracked even deep within the interior of large, dense systems. Such a capability yields a great advantage in the exploration of systems such as ours, where the inability to visualise internal dynamics and particle distributions has limited past studies [38, 72].

Although PEPT tracks a single particle, for systems in a steady state the principle of ergodicity allows the extraction of data pertaining to the system as a whole through appropriate time-averages, as shown in detail in our reference [70]. Indeed, PEPT has been successfully used to determine steady-state density and temperature distributions [73], velocity fields [74, 75] and segregation patterns [76] as well as numerous additional important, whole-field quantities in a diverse range of systems [77–79]. In order to obtain useful data from binary systems such as ours, it is simply necessary to repeat every experiment using a tracer of each species, combining the time-averaged data from each separate run [80]. Provided below is a brief explanation of the manner in which the quantities most pertinent to the current study may be calculated from PEPT data.

2.2.1. Residence fractions, particle distributions and segregation

The distribution of particles within our system can be determined from PEPT data as follows: firstly, the experimental volume is divided into a series of equally-sized three-dimensional 'cells'. The amount of time spent by our tracer in each of these cells can then be determined and divided by the total duration of the run, thus assigning each individual cell a fractional residence time, τ. For our steady-state system, the average fraction of time, τ, spent by our tracer in a given cell is equivalent to the average fraction of the system's particles which can be expected to occupy this cell at any given point in time. In other words, for any region of the system, τ is directly proportional to the local packing fraction, η. Knowing this, for a bidisperse system it is possible to determine ϕ_i, the relative fractional concentration of a given species '*i*' in a given cell, from the simple relation $\phi_i = \frac{\tau_i}{\tau_i + \tau_j}$, where '*j*' is the binary system's second particle species and τ_j is the residence fraction of this species in the same cell. Hence, for adequately small cells, it is possible to reproduce the average particle distribution within the system as a whole, and thus to visualise the steady-state segregation patterns exhibited–see, as an example, figures 4, 5. Note that, in these images, data has been depth-averaged through the cartesian *y*-direction to produce a 2D plot in order to make the results more easily comprehensible. In order to allow the depth-averaged images used throughout this manuscript to be easily interpreted, a simple pictorial representation of the correspondence between the three-dimensional system explored and the two-dimensional 'projections' exhibited here may be seen in figure 3. It is also possible to additionally average through the vertical (z) direction in order to produce one-dimensional concentration profiles, such as those shown in figure 12.

Using the partitioned particle concentration values described above, it is also possible to construct a single scalar value which can be used to easily quantify the extent of segregation exhibited by a system as a whole. In this

paper we use I_s, the *segregation intensity* [36, 81], which is defined as:

$$I_s = \frac{1}{I_s^{\max}} \left[\frac{\sum_{n=1}^{n=N_c} (\phi_i^n - \phi_i^m)^2}{N_c} \right]^{\frac{1}{2}}. \quad (1)$$

Here, N_c is the total number of cells within the system, ϕ_i^n is the fractional concentration of species i in the n^{th} cell and ϕ_i^m the mean concentration of species i particles for the system as a whole. $I_s^{\max}$ is equal to the 0.5, the maximum of the term $\left[\frac{\sum_{n=1}^{n=N_c} (\phi_i^n - \phi_i^m)^2}{N_c} \right]^{\frac{1}{2}}$ for our current system, thus acting as a normalisation constant such that an I_s value of 1 denotes a completely segregated state, while $I_s = 0$ corresponds to a perfectly mixed system.

2.2.2. Velocity Vector Fields

In order to calculate velocity vector fields, the system volume is again divided into a series of three-dimensional cells. For a given cell, the sum of the x-, y- and z-velocities corresponding to all data points whose position vectors fall within this cell's spatial domain are summed. Hence, an average velocity vector associated with each individual cell can be determined. While it is possible to obtain a two-dimensional velocity field simply by taking a 2D projection through the y-direction, as with the particle concentration fields decribed above, with the velocity fields we are primarily interested in the free-flowing upper layer of the granular bed as opposed to the lower, bulk region which simply undergoes solid-body rotation, with little or no axial motion. As such, we may exploit the fully-three-dimensional nature of PEPT data and instead average only over cells corresponding to the system's downward-flowing layer. A pair of velocity vector fields produced in this manner may be seen in figure 8. Here, the orientation of the arrows shown indicates the direction of the net flow in a given region of the system, and the arrow length indicates the magnitude of the average flow velocity through this region.

2.2.3. Fluctuation energy distribution

The determination of the variation in *fluctuation energy*, $\tilde{E}$, throughout our system allows us to experimentally test the theory of Fan and Hill [52, 53]. Fan and Hill predict that, due to the squeeze-expulsion process detailed in section 1.1, a net migration of smaller particles to regions of lower fluctuation energy should be observed, with a corresponding net flux of larger particles toward higher-$\tilde{E}$ regions.

The fluctuation energy vector for a given region of a system is defined as:

$$\tilde{E}_i = \frac{\sum_{n=1}^{N} (\bar{v}_i - v_i^n)^2}{N} \; (i = x, y, z) \quad (2)$$

where the index i denotes the velocity component for which $\tilde{E}$ is calculated, $\bar{v}_i$ is the mean i-velocity for the chosen region and v_i^n is the i-velocity for the n^{th} particle of the N total particles in this region.

By once again partitioning our experimental volume into a series of equal-volume cells, it is possible to map the variation of $\tilde{E}$ within our system–see, for an example, figure 6. In the present work, we focus on the axial (x) component of $\tilde{E}$, as it is the motion and resultant distribution of particles along this direction which forms the focus of our work. It is worth noting, however, that the distributions of the *total* fluctuation energy ($\tilde{E}_{tot} = \tilde{E}_x + \tilde{E}_y + \tilde{E}_z$) follow a highly similar pattern in all instances tested.

3. Results and discussion

3.1. Generalisation of CC Segregation

The results of Gonzalez *et al* [66] clearly show that strong axial segregation can be induced through the use of a single rotating drum split symmetrically in the axial direction into a region possessing a (convex) pentagonal internal cross-section and a region possessing a (concave) pentagramal geometry. However, the paper failed to address a critical issue: can the proposed segregation mechanism be generalised to *all* convex-concave pairings? Or is it limited, for instance, to pairings where both convex and concave members possess the same number of vertices? Or indeed does it only apply for the specific pentagon-pentagram pairing previously tested?

To address this issue, we tested various combinations of convex and concave drums, using all possible permutations[3] of the polygonal geometries shown in figure 2. Figure 4, shows the particle distributions observed for triangle-pentagram and hexagon-hexagram pairings. In each instance, the tendency of small particles to occupy concave regions and larger particles to dominate convex regions is clearly observable. In fact, the same holds true for all convex-concave pairings, although the *strength* of segregation varies considerably for different combinations, as will be discussed in detail in section 3.4.

[3] Note that while a qualitative visual assessment of the segregated state of each geometrical combination was possible, due to the time and financial constraints associated with PEPT, a full, quantitative analysis was not possible for all permutations.

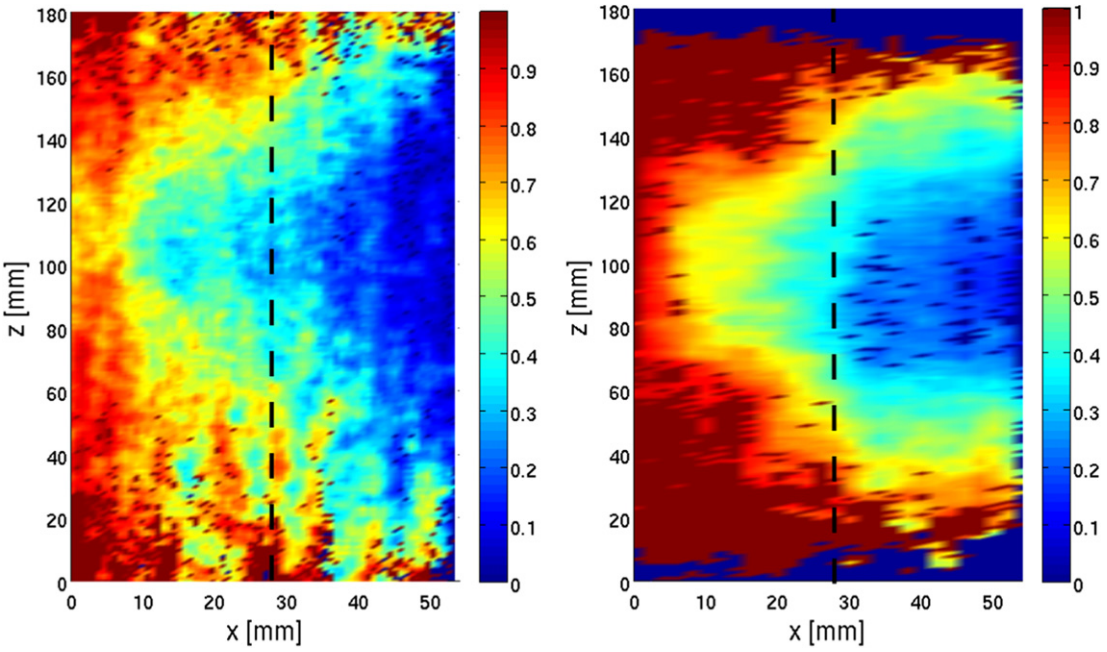

Figure 4. Two-dimensional plots showing the steady-state spatial variation of the fractional concentration of large particles, ϕ_l. The data shown is depth-averaged through the y-direction in order to produce a two-dimensional concentration field in the x-z plane where x is the axial and z the vertical direction. Results are shown for drums split symmetrically into adjacent regions possessing (convex) triangular and (concave) pentagramal internal cross sections (left) and possessing (convex) hexagonal and (concave) hexagramal cross-sections (right). In each case, the left side of the drum ($0 < x < 27$ mm) is convex and the right ($27 < x < 54$ mm) concave. A value $\phi_l = 1$ denotes a region of space occupied exclusively by particles of the larger (l) species, while $\phi_l = 0$ corresponds to a volume dominated entirely by particles of the smaller (s) species. Dashed lines represent the axial positions of the interfaces between regions of differing geometry.

It is additionally worth noting that the CC mechanism is found to persist in spite of considerable variations in the length and diameter of the drum used as compared to the original experiment, as well as for different particle sizes and materials, volume fractions, fill heights and rotation rates. Our systems are also found to obey the CC mechanism irrespective of the relative cross-sectional areas of the convex and concave regions, with larger particles migrating to convex regions for all systems explored, both for $A_{\text{convex}} > A_{\text{concave}}$ and $A_{\text{convex}} < A_{\text{concave}}$.

In short, our data strongly suggest that CC segregation is indeed a robust and generalisable phenomenon, and not simply limited to a few special cases. This result is potentially of value to researchers or industrialists who may wish to exploit the mechanism in order to selectively separate materials, as it shows that the segregation process is not reliant on overly specific constraints regarding the choice of suitable geometries.

3.2. Inducing and directing axial segregation

Thus far, we have only discussed CC segregation in the simple, symmetric two-region geometry discussed above. However, our results strongly imply that the mechanism will apply for an arbitrary number of adjacent convex and concave regions, allowing the creation of an effectively limitless variety of segregation patterns. Examples may be seen in figure 5, where the use of, respectively, three and six alternating convex and concave axial regions produces clear axial banding.

Our results clearly demonstrate that, at least for the relatively narrow axial segements discussed here, large and small particles will migrate, respectively, to the convex and concave regions of the system, irrespective of the total number of such regions and their particular placement. In other words, this observation allows us a *predictive knowledge* of the specific segregation pattern produced by a given system. This is in stark constrast to the 'normal' axial banding observed in axially homogeneous systems, where the large and small particle bands produced are known to be metastable [26], with their widths and positions varying over time. The specific locations and sizes of the bands are also found to be irreproducible over identical repeated runs [82, 83].

Axially banded granular assemblies are also known to undergo a process of *coarsening* [84–86] whereby, over relatively long periods, individual bands merge, resulting in a logarithmic decay of the number of bands within the system. Such coarsening is, however, seemingly absent from our systems. The coarsening effect is known to occur over time periods corresponding to the order of thousands of drum revolutions [85, 86], yet the bands observed in our systems are invariably observed to remain stable over the 3000–6000 revolutions to which they

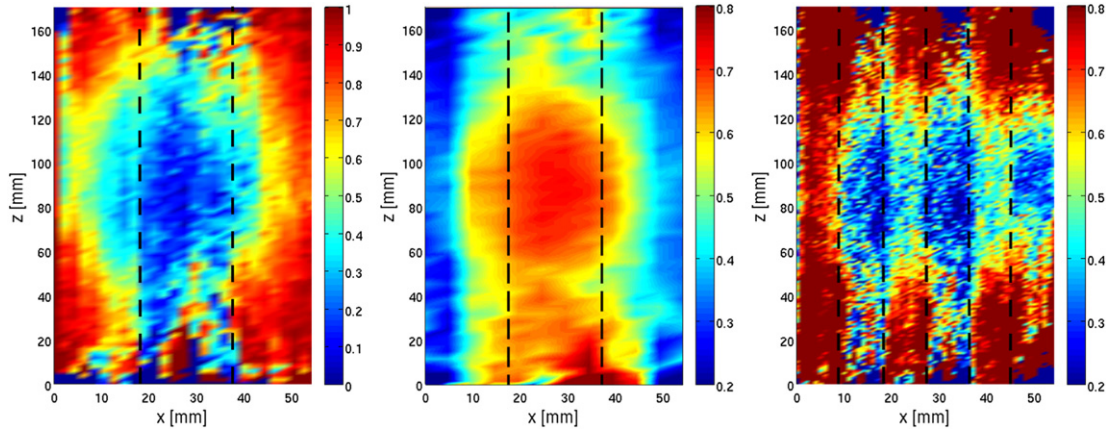

Figure 5. Two-dimensional depth-averaged ϕ_l-distributions for three differing arrangements of convex and concave sections. In all images shown, dashed lines represent the axial positions of the interfaces between regions of differing geometry. Left: a system of total axial length 54 mm divided axially into three regions of equal width with the outer regions possessing a (convex) pentagonal internal geometry and the central region a (concave) pentagramal geometry. Centre: a 54 mm system divided into three equal-width regions in a concave-convex-concave arrangement of triangular and hexagramal geometries. Note that, unlike in figure 4 and indeed the other panels in the current figure, the concave region possesses a higher cross-sectional area than the convex regions, yet large particles continue to migrate towards the convex region, as expected from the CC mechanism. Right: a 54 mm system subdivided into six 9 mm segments in an alternating convex-concave arrangement of pentagonal and pentagramal sections starting at $x = 0$ with a region possessing a convex internal geometry. Note that the degree of segregation observed in the 6-band case is somewhat reduced as the size of the individual axial segments becomes comparable to the l-particle diameter.

are exposed. Indeed, we do not observe even the beginnings of the coarsening process (i.e. the widening or narrowing of individual bands [86]). Additional tests in which the system is left to rotate continuously for a 24-hour period (36000 revolutions) similarly show no signs of coarsening.

The known positions and stability of the axial bands present in our system means that it is possible to design systems in such a manner that we can in essence '*choose*' the segregation pattern to be produced. Clearly, such an ability to deliberately control the direction of segregation within a system may be useful in any practical application where the sorting of grains or particles is required.

3.3. Kinetic stress and segregation

As briefly noted in section 1.1, and discussed extensively in our references [52, 53, 65], it has been suggested that the presence of shear rate gradients within a system may modify its segregation trends. These shear rate gradients manifest themselves as differences in the magnitudes of local velocity, and hence kinetic energy, fluctuations [87] exhibited by the system. It is found that, for dense systems, *larger particles* will segregate towards regions of *greater fluctuating energy*, $\tilde{E}$.

Using PEPT, it is possible to measure the average fluctuation energy at any point within our experimental volume, meaning that we are able to construct a two-dimensional 'heat map' of our system which–unlike with many conventional techniques–accounts for the motion of particles throughout the *entire depth of the bed*, as opposed to simply those near the extremeties of the system. Thus it is possible for us to directly compare the axial distribution of particles within our system to the variation in $\tilde{E}$, and hence assess, at least on a qualitative level, the validity of the above-described theory.

In order to determine the presence (or indeed absence) of kinetic-stress-driven segregation in our systems, we study a series of (convex-concave) pentagon-pentagram drums of varying total axial length, l, with, in all cases, $L_{\text{convex}} = L_{\text{concave}} = \frac{L}{2}$. Due to the non-uniform geometry of these systems, one would naturally expect flow to invariably be more turbulent in the concave regions of a system, resulting in an increased fluctuating kinetic energy in these areas relative to adjacent convex segments. This expectation is indeed vindicated by our results, as exemplified in figure 6, which demonstrates the protoypical $\tilde{E}$ distribution for all convex-concave systems. Note that, in this figure, we consider specifically the x-component of the fluctuation velocity, $\tilde{E}_x$, as this is the component which will most directly influence *axial* segregation. It is nonetheless worth mentioning that $\tilde{E}_y$, $\tilde{E}_z$ and hence the total fluctuation energy, $\tilde{E}$, all exhibit similar spatial distributions.

From figure 6 we also see a particularly marked increase in the fluctuating kinetic energy at the interface between the convex and concave regions of the system and at the axial extremeties, where friction with the system's end-walls will produce shear, and hence induce a local increase in $\tilde{E}$ [65, 88]. Superimposed on the 'heat map' of figure 6 are the axial particle distributions for the large (l) and small (s) components of the granular bed housed within the drum, as well as the total particle distribution. Note the localised peaks in the total particle concentration near the system's left-hand end wall, and at the interface between convex and concave regions of

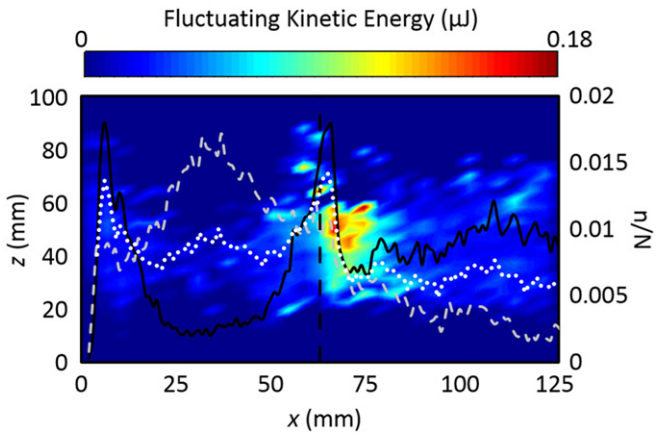

Figure 6. Two-dimensional plot showing the spatial distribution of the x-component of the fluctuation velocity, $\tilde{E}_x$ for a system of length $L = 126$ mm, overlayed with one-dimensional, time-averaged particle distributions. Here, n represents the average number of particles of a given species in a given axial region and N the total number of particles of this species in the system as a whole. The solid black line corresponds to the distribution of large (l) particles, with the dashed gray line representing the small (s) species and the dotted white line the distribution of *all* particles within the system. The lower total particle concentration on the right-hand side of the figure is a consequence of the reduced cross-sectional area of the concave region of the system. The data shown correspond to a system of total lenth 126 mm divided into two equal-width convex (pentagonal) and concave (pentagramal) sections whose interface lies at the system's axial centre ($x = 63$ mm). The position of this interface is marked by a vertical, dashed black line.

the drum. It is well known [89] that boundary effects can induce changes in the local angle of repose of a granular bed, and hence induce localised 'heaping'. It is interesting to observe the absence of such heaping for the system's right-hand wall, corresponding to the concave section of the drum. This is potentially due to the greater fluctuation in the velocties of particles in the concave geometry [66] preventing the formation of a heap. Although external to the aims of the current study, a more detailed analysis of the heaping phenomena within convex-concave systems is worthy of future research. Most important for the present study is the observation of a *strong correlation* between regions of high $\tilde{E}$ and the local concentration of l particles and, conversely, a preponderance of s particles where the flow is most laminar.

The above results provide a significant measure of support for the theory of Fan and Hill [52, 53]. In particular, the existence of a region of larger particles near the system's wall draws a strong parallel with the observations of Fan and Hill for a simulated chute flow geometry [52]; the segregation observed at the interface between concave and convex drum segments, meanwhile, is somewhat analogous to their observations of segregation in a split-bottom shear cell [58].

While the above-described results provide support for the mechanism of Fan and Hill, they are in fact directly contradictory to the behaviours expected from the CC mechanism. In other words, it seems that, for relatively elongated systems–or, more accurately, systems in which *each individual convex/concave segment* is relatively elongated–kinetic-stress-induced segregation is decidedly dominant over the CC mechanism.

In the next section, we will discuss more precisely the range of system lengths for which each (if either) mechanism is dominant, and demonstrate how the competition between the two can be exploited in order to control the mixing and segregative behaviours of a system.

3.4. Interactions between competing mechanisms

3.4.1. Area modulation versus CC segregation

A final question to resolve regarding the validity of the relatively newly observed CC segregation mechanism is whether the segregation patterns observed can be simply explained by the area modulation mechanism proposed by Zik *et al* [50]–i.e. is the observed particle separation truly due to a change of the specific geometries, or simply due to the corresponding variation in the cross-sectional area of the different polygons tested?

Firstly, we note that evidence of the segregation mechanism of [50] is clearly present in our system; figure 7, for instance, shows that a system comprising exclusively cylindrical sections of differing diameter will produce segregation, as expected by Zik *et al* In the leftmost panel of this figure, which shows simply the total, depth-averaged packing density within the system, we can clearly see evidence of the differing repose angles for regions possessing smaller and larger cross-sectional areas. In the right-hand panel, meanwhile, we show the resultant steady-state segregation pattern.

Interestingly, this mechanism is not limited to purely cylindrical systems. For all tested convex-convex and concave-concave (as opposed to convex-concave) combinations, the (more mobile [90, 91]) large particles were invariably observed to migrate towards regions possessing smaller cross-sectional areas and correspondingly

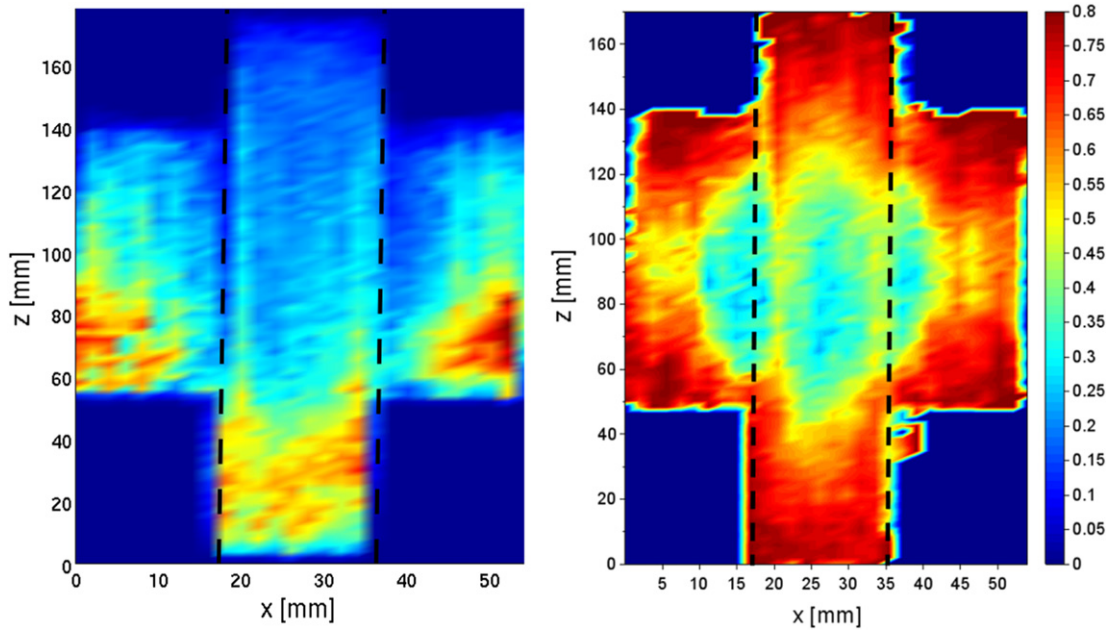

Figure 7. Left: time-averaged, two-dimensional packing density distribution for both small and large components of a bed with a geometry comprising two 18 mm width cylindrical segments of internal diameter 150 mm and one central cylindrical segment of equal width but with diameter 250 mm. Right: concentration distribution for the large particle component of the system described in (a). In each of the images shown, dashed lines represent the axial positions of the interfaces between regions of differing geometry.

lower angles of repose–a pleasing indicator of the generality of the findings of Zik *et al* which, to the best of the authors' knowledge, has not been previously demonstrated.

When convex-concave systems are considered, however, numerous counter-examples to the expectations of Zik *et al* [50] are observed, demonstrating unequivocably that the CC segregation is not simply due to differences in cross-section between dissimilar axial regions. In the images presented in figures 4 and 3, for instance, we see a distinct prevalence of large particles in drum segments with a *larger cross-sectional area*–the exact inverse of our expectations from the above discussion. This reversal in the sense of the observed segregation provides a direct demonstration that CC segregation, in these instances, is not only distinct from but also decidedly *dominant over* that due to differences in cross-sectional area. In actuality, the dominance of the CC mechanism over the area modulation mechanism posited in [50] is found to persist for all convex-concave systems explored.

The reasoning behind this result may perhaps be understood by analysing axial velocity fields such as those presented in figure 8 for mixed convex-concave geometries in which the convex regions also possesses larger cross-sectional areas than their concave counterparts. In these images, we can clearly observe the interplay between the two competing segregation mechanisms. Specifically, in the upper regions of the system (i.e. at the start of the free-flowing layer) where cross-sectional area-related differences in angle of repose are most pronounced, we see an initial net flow of *l* particles from the larger, convex sections to the smaller, concave sections, as expected from [50]. However, in the lower portion of the flowing region, we observe a reversal in the direction of axial transport as larger particles cascade into the unoccupied regions of the convex drum segments–the CC mechanism. Since it is at the bottom of the flowing layer that particles then become 'locked in position' as they enter solid-body motion, it stands to reason that the CC process plays the crucial rôle in determining the direction of axial segregation within the system.

While one might intuitively expect that an increased ratio, $\frac{A_{\text{convex}}}{A_{\text{concave}}}$, of the cross-sectional areas of the drum's convex and concave regions would result in greater competition between the two mechanisms and hence a reduced net segregation, in practice, the opposite seemingly holds true. Figure 9 shows the variation of the normalised segregation intensity, I_s (as described in section 2.2.1), with $\frac{A_{\text{convex}}}{A_{\text{concave}}}$.

Figure 9 demonstrates that, as mentioned previously, the specific combination of convex and concave shapes used strongly influences the degree of segregation observed. This is a potentially important observation, as it demonstrates the the possibility that one may *deliberately alter* the degree to which a system segregates through a simple change in the drum geometry, leaving all other parameters—e.g. fill height, rotation rate, particle size and material—unaltered. Such an ability may be useful in industry, for instance, where a variation in these other

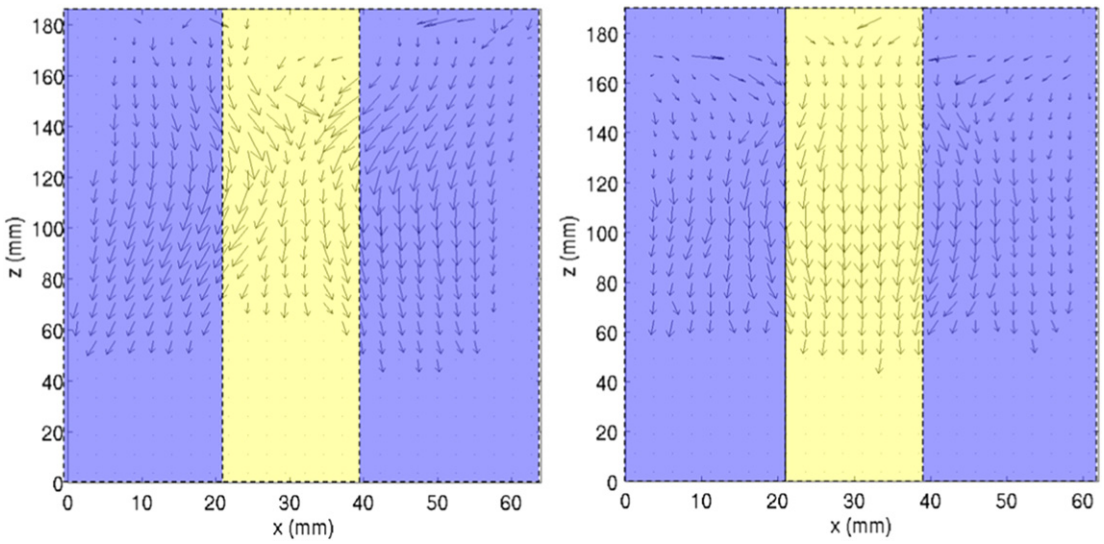

Figure 8. Two-dimensional, depth-averaged velocity vector fields corresponding to the free-flowing regions of the systems presented. Data is shown for a convex-concave-convex arrangement of triangular and pentagramal drum segments (left) and a concave-convex-concave arrangement of pentagonal and pentagramal sections (right). For both cases shown, $A_{\text{convex}} > A_{\text{concave}}$. In each image, the drum's inner segments are shown in yellow and outer segments in blue, emphasising the interfaces between differing regions, where the orientation of axial flow is most relevant. Data in this figure are only shown for the system's free flowing layer, meaning that data points are not included for the (solid-body) region near $z = 0$.

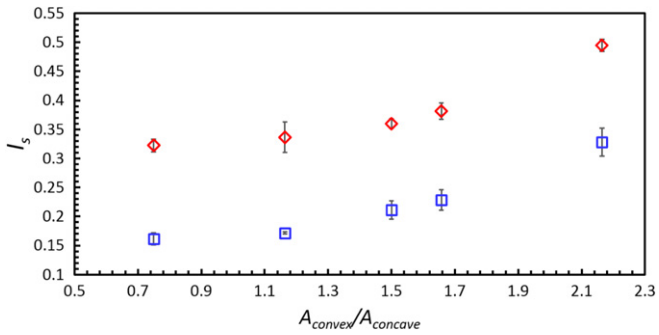

Figure 9. Segregation intensity, I_s, as a function of $\frac{A_{\text{convex}}}{A_{\text{concave}}}$, the relative cross-sectional area of convex and concave drum segments. Data are shown for drums divided axially into three equal segments each of width 18 mm in both convex-concave-convex (red diamonds) and concave-convex-concave (blue triangles) arrangements. The various values of $\frac{A_{\text{convex}}}{A_{\text{concave}}}$ presented are achieved using combinations of the convex and concave internal geometries pictured in figure 2.

parameters may be difficult and/or undesirable—a change in particle properties will require an alteration of the product being processed, while a change in filling fraction will likely affect efficiency.

The trend between I_s and $\frac{A_{\text{convex}}}{A_{\text{concave}}}$ observed in figure 9 can potentially be explained as follows: CC segregation is driven by the increased peak velocity of particles in concave geometries as compared to those in convex geometries [66]. However, our results additionally show that the absolute flow velocity in a concave region is seemingly dependent on its convex partner—a pentagram-pentagon pairing exhibits faster flow than an equivalent pentagram-triangle pairing, for instance. In fact, although it is difficult to fully quantify due to the ill-defined boundaries of the free flowing layer in a given system combined with our limited spatial resolution, our results show a positive correlation between the surface flow rate of a given concave drum segment and the cross-sectional area of its convex counterpart. This makes physical sense—a smaller convex volume will possess less free space to accommodate an influx of (large) particles, thus more quickly restricting, and hence slowing, the surface flow. Since CC segregation is induced by the rapid flow of large particles into unoccupied regions of convex geometry, it seems logical that a faster flow (due to a larger convex area) will result in more pronounced segregation, and vice-versa.

The above hypothesis may also explain—at least in part—why, as demonstrated in figure 9, a three-segment concave-convex-concave arrangement will display a markedly reduced degree of segregation compared to an

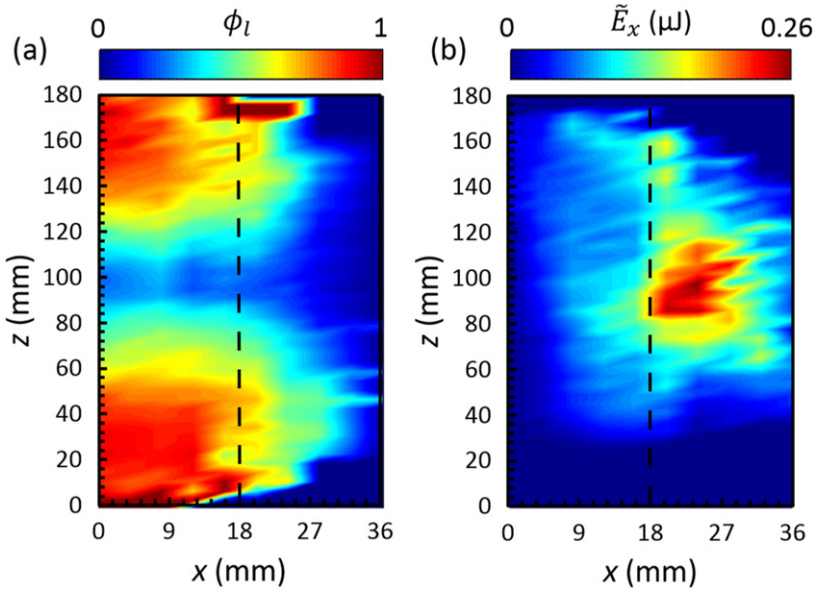

Figure 10. (a) Two-dimensional concentration field showing the spatial variation in the relative local fraction of large particles, ϕ_l, for a convex-concave system of length 36 mm. (b) Spatial variation of the axial component of the local mean fluctuating kinetic energy, $\tilde{E}_x$, for the same system. The system shown is divided symmetrically into a convex pentagonal and concave pentagramal region, with the interface between these regions marked by a dashed black line.

equivalent convex-concave-convex ordering: in the latter situation, particles in the single concave segment are provided with two adjacent convex sections into which they may cascade, facilitating a rapid flow. In the former, meanwhile, large particles from two concave regions are effectively channeled into a single convex region, resulting in a reduced avalanche speed in much the same manner as a lane closure will slow the flow of traffic on a busy highway.

To summarise the above discourse, for cases in which convex and concave drum segments possessing differing cross-sectional areas coexist in a single system, the geometry-based CC segregative mechanism will act in opposition to segregative processes arising due to differences in drum area. However, our results show the CC segregative mechanism remains emphatically dominant across the entire range of parameter space explored, strongly suggesting that segregation driven purely by differences in area will only be apparent in convex-convex or concave-concave systems.

3.4.2. CC segregation versus kinetic-stress-driven segregation

As noted in section 3.3, the relative strength of the CC mechanism [66] and the kinetic-stress-induced mechanism proposed by Fan and Hill [52, 53] in a convex-concave system is highly dependent on the length of the individual drum segments used. Specifically, in shorter systems the CC mechanism is seemingly dominant, while in longer systems the kinetic-stress-driven process is the the primary driving force behind segregation. This is likely due to the fact that the CC mechanism is only active at the interface between convex and concave segments, and hence exerts a strong but short-range effect, while Fan and Hill's kinetic stress mechanism is influential over a longer range. In other words, our results strongly imply the former to be a *local* effect, and the latter to apply *globally*.

Evidence to this effect may be seen by comparing figures 6 and 10; while the former, which is discussed at length in section 3.3, shows larger particles to primarily inhabit regions of higher fluctuation energy (as expected for kinetic-stress-driven segregation), in the latter there exists little or no correlation between the high-$\tilde{E}$ regions and the areas of high *l*-particle concentration. Rather, we see a definite preponderance of *l* particles in the (*less* turbulent) convex region, as expected from CC segregation.

Figure 11 provides a more direct demonstration of the influence of drum length–or, more accurately segment length (as a long drum split into many short segments will still obey CC segregation). For small segment lengths, L_{seg}, segregation is seemingly driven by the CC mechanism, with a clear net migration of *l* particles to the system's convex regions (represented in figure 11 by a positive I_s value). For the longest systems tested, meanwhile, we see a distinct tendency for larger particles to occupy concave regions, i.e. those possessing higher fluctuation energies. Segregation in this direction is represented in figure 11 by a reversal in the sign of I_s, with the magnitude of this value corresponding to the observed strength of segregation. Although quantitative PEPT data is only available for the pentagon-pentagram systems shown in figure 11, visual observations confirm, on a

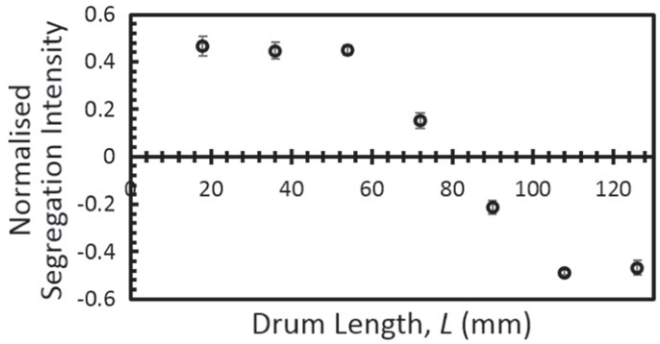

Figure 11. Plot of the segregation intensity, I_s, as a function of drum length for a series of (convex-concave) pentagon-pentagram systems with fixed $F = 0.4$ and $V_l = V_s$. In all cases, the drum is divided into two, adjacent, equally-sized regions, i.e. $L_{\text{seg}} = \frac{1}{2}L$. Positive (negative) I_s values represent systems in which large particles predominantly occupy convex (concave) regions.

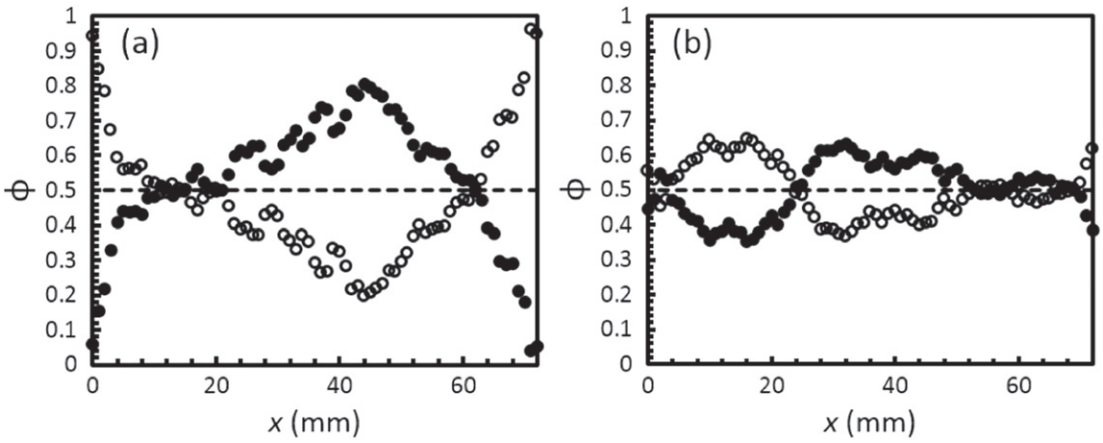

Figure 12. Axial variation of the local relative volume fraction, $\phi_{s,l}$, of small (open circles) and large (closed circles) particles for (a) an axially uniform cylindrical system and (b) an axially inhomogeneous pentagon-pentagram system, each with $L = 72$ mm, $F = 0.4$ and $V_l = V_s$. The system's mean volume fraction, ϕ_m, is represented by a dotted line in both cases.

qualitative level, that the observed reversal in the sense of segregation with increasing L_{seg} occurs for all convex-concave pairings available.

Perhaps most notable from figure 11 is the marked drop in the degree of segregation for intermediate drum lengths, where the two opposing segregation mechanisms possess comparable strengths; specifically, we observe a more than three-fold reduction in the magnitude of I_s as compared to the extremal cases. Figure 12 shows that by exploiting a system geometry such as ours to counterpose two distinct segregative processes, it is actually possible to achieve *better mixing* than is attained in a conventional, cylindrical system under otherwise identical conditions. Particularly noteworthy in figure 12 is the marked reduction in end-wall segregation—likely due to the introduction of CC segregation, which is not directly reliant on effects due to friction and/or shear. This is a pleasing result, as end-wall segregation is often observed even in systems which are otherwise non-segregative in the axial direction [92, 93].

It should be noted that the construction of our system is such that the drum length, L, can only be varied in discrete 18 mm intervals if symmetry (i.e. $L_{\text{convex}} = L_{\text{concave}}$) is to be maintained. With more sensitive adjustment, it may in fact be possible to cause the two mechanisms to *entirely cancel* and hence induce near-perfect mixing–a potential boon for industry [94–96]. Such an equilibration may also potentially be achieved by varying the specific internal geometries used so as to alter the relative change in fluctuation energy between the two halves of the drum, for instance. The example shown nonetheless displays an impressive increase in the observed degree of mixing, with $I_s = 0.37 \pm 0.02$ for the uniform cylinder compared to $I_s = 0.16 \pm 0.01$ for the convex-concave geometry.

Table 1. Table showing, for each combination of internal geometry and individual segment length, the dominant segregation mechanism or mechanisms and the type or, where relevant, direction of the segregation produced. For instance, 'Large →' high-A' denotes a net migration of large particles to regions possessing greater cross-sectional areas. The segment length refers to the length of an individual convex or concave axial segment of the rotating drum system and, for generality, is normalised by d_l, the diameter of the large (l-species) particles used in this study. The various segregation mechanisms (CC, kinetic stress, area modulation) are detailed in section 1.1.

		Segment Length		
		Short $\left(\frac{L_{\text{seg.}}}{d_l} \lesssim 13.5\right)$	*Intermediate* $\left(13.5 \lesssim \frac{L_{\text{seg.}}}{d_l} \lesssim 27\right)$	*Long* $\left(\frac{L_{\text{seg.}}}{d_l} \gtrsim 27\right)$
Internal Geometry	*Convex-Concave*	CC Large → Convex	CC / Kinetic Stress Weak Segregation / Mixing	Kinetic Stress Large → Concave
	Convex-Convex	Area Modulation Large → High-A	Area Modulation Large → High-A	Undefined / Other Metastable
	Concave-Concave	Area Modulation Large → High-A	Area Modulation Large → High-A	Undefined / Other Metastable

3.4.3. A summary of competing mechanisms

We conclude the current section by the summarising dominant segregation mechanisms expected for each of the various permutations of drum segment length and internal geometry explored here.

For systems comprising any arbitrary number of *short* drum segments with alternating *convex-concave* geometry, segregation will be driven by the CC mechanism, with stable bands of large particles forming in regions possessing convex internal geometries.

For similar systems possessing *solely convex* or *solely concave* geometries, the area-modulation mechanism of Zik *et al* [50] is dominant, causing larger particles to migrate to regions of lower cross-sectional area. The same mechanism seemingly holds also for systems of *intermediate* length, albeit with a reduced overall degree of segregation.

For relatively *long, convex-concave* systems, the system's segregative behaviours are seemingly determined by the kinetic-stress-driven mechanism of Fan and Hill [52, 53], with large particles forced towards regions of high fluctuation energy. For *convex-concave* systems of *intermediate* length, meanwhile, competition with the CC mechanism [66] results in a considerably reduced net segregation.

Finally, for *long, concave-concave* or *convex-convex* systems, there exists no clear evidence of any of the three mechanisms discussed in this paper, aside from the presence of end-wall segregation due to the localised shear in the vicinity of the system's lateral boundaries. Rather, the system seemingly exhibits, in its central bulk, the randomly placed, metastable bands typically observed in long, purely cylindrical systems [26, 82, 83]. This observation is not overly surprising, as the segments are too long for the relatively localised mechanism of Zik *et al* to play a significant rôle, and–due to the absence of strong differences in shear and/or turbulence between neighbouring regions as is observed in *convex-concave* systems—not conducive to significant kinetic-stress-driven segregation. Although a detailed discussion of the behaviours observed for these systems is beyond the scope of the current work, it is certainly a matter worthy of future study.

For ease of reference, the information given above is presented in a more succinct form in table 1.

4. Conclusions

In this paper, we have investigated the presence of, and interactions between, three distinct mechanisms, each of which has been proposed as an explanation for the axial segregation of granular media in a horizontally rotating drum.

We have provided evidence of the existence of each of these mechanisms in the systems studied, including a generalisation of the theory of Zik *et al* [50] to systems possessing non-circular internal geometry, a generalisation of the 'CC mechanism' of Gonzalez *et al* [66] to arbitrary convex-concave geometries and, perhaps most importantly, a *first experimental validation* of the model of Fan and Hill [52, 53] in the rotating-drum geometry.

The local, boundary-driven effects corresponding to the CC [66] and area modulation [50] mechanisms observed within this study are yet to be included in any existing continuum models of granular flow. The demonstration provided here of the *significant influence* of these effects on the flow dynamics of our systems therefore presents an open challenge to the theoretical community and, as such, provides significant scope for future research.

We have explored the complex interactions between the three mechanisms studied under a variety of geometric constraints, showing the ranges of validity for each mechanism, and establishing which, if any, of the three may be expected to dominate a system's behaviour for a given drum geometry.

Further, we have shown several novel manners in which the geometry of a system may be deliberately 'tuned' in order to exploit the individual mechanisms studied and indeed their competitive and cooperative interactions such that the segregative behaviours of a granular system may effectively be *predicted* and hence *controlled*. Most notably, we have demonstrated that by partitioning a system into a series of thin segments possessing differing internal geometries, we are able to produce predetermined, stable axial segregation patterns—i.e. it is possible to *actively choose* the regions of a system to which a particular particle species will migrate. Such an ability clearly has practical applications in industry. Moreover, if our findings here can be generalised to different flow geometries, the ability to re-direct granular flow may potentially be useful in other fields, e.g. redirecting the most destructive parts of avalanche—or debris—flows in order to protect populated areas [97]. We have also shown that it is possible to countervail the action of a given segregative process using another, opposing mechanism, allowing a significant increase in the degree of mixing exhibited by a binary system. The ability to achieve mixing in systems such as ours is highly desirable in many industrial processes, but also notoriously difficult to achieve using conventional techniques [2, 5, 27, 29, 98].

Finally, and perhaps most importantly, our results as a whole clearly highlight the fact that the axial segregation of rotated granular systems cannot be explained by a single mechanism, as is often assumed both in past and contemporary studies. Rather, there seemingly exist multiple processes by which axial segregation may occur, with the active mechanism–or mechanisms–being dependent on the specific conditions to which a system is exposed. As such, the only way to *fully understand* axial segregation is to determine the regions of parameter space in which each individual mechanism is dominant, and how they interact when the dominance of any one particular process is not clearly established. Although the current work concerns only three of a currently undetermined number of relevant mechanisms and deals specifically with the effects of system geometry, it nonetheless represents an *important first step* towards the ultimate goal of developing a *full, predictive knowledge* of axial segregation.

Acknowledgments

This project was funded through the Dutch Technology Foundation STW via Project No. 13472 564 FQ STW, 'Shaping-Segregation.', the NWO-STW VICI Grant No. 10828 and the University of Birmingham's Hawkesworth Scholarship, provided by the late Dr Michael Hawkesworth.

References

[1] de Gennes P-G 1999 Granular matter: a tentative view *Rev. Modern Phys.* **71** S374
[2] Jaeger H M, Nagel S R and Behringer R P 1996 Granular solids, liquids, and gases *Rev. Mod. Phys.* **68** 1259
[3] Duran J 2000 *Sands Powders, and Grains* (Berlin: Springer)
[4] Jaeger H M, Nagel S R and Behringer R P 1996 Granular solids, liquids, and gases *Rev. Mod. Phys.* **68** 1259–73
[5] Metcalfe G, Shinbrot T, McCarthy J J and Ottino J M 1995 *Avalanche mixing of granular solids*
[6] McCarthy J J, Shinbrot T, Metcalfe G, Eduardo Wolf J and Ottino J M 1996 Mixing of granular materials in slowly rotated containers *AIChE J.* **42** 3351–63
[7] Ristow G H 1996 Dynamics of granular materials in a rotating drum *Europhys. Lett.* **34** 263
[8] Gray J M N T 2001 Granular flow in partially filled slowly rotating drums *J. Fluid Mech.* **441** 1–29
[9] Bridgwater J 1976 Fundamental powder mixing mechanisms *Powder Technol.* **15** 215–36
[10] Khakhar D V, McCarthy J J, Shinbrot T and Ottino J M 1997 Transverse flow and mixing of granular materials in a rotating cylinder *Phys. Fluids* **9** 31–43
[11] Juarez G, Chen P and Lueptow R M 2011 Transition to centrifuging granular flow in rotating tumblers: a modified froude number *New J. Phys.* **13** 053055
[12] Lehmberg J, Hehl M and Schügerl K 1977 Transverse mixing and heat transfer in horizontal rotary drum reactors *Powder Technol.* **18** 149–63
[13] Van Puyvelde D R, Young B R, Wilson M A and Schmidt S J 1999 Experimental determination of transverse mixing kinetics in a rolling drum by image analysis *Powder Technol.* **106** 183–91
[14] Khakhar D V, Orpe A V and Hajra S K 2003 Segregation of granular materials in rotating cylinders *Physica* A **318** 129–36
[15] Chaudhuri B, Muzzio F J and Tomassone M S 2006 Modeling of heat transfer in granular flow in rotating vessels *Chem. Eng. Sci.* **61** 6348–60
[16] Kwapinska M, Saage G and Tsotsas E 2008 Continuous versus discrete modelling of heat transfer to agitated beds *Powder Technology* **181** 331–42
[17] Green D W *et al* 2008 *Perry's Chemical Engineers' Handbook* vol 796 (New York: McGraw-Hill)
[18] Clément E, Rajchenbach J and Duran J 1995 Mixing of a granular material in a bidimensional rotating drum *Europhys. Lett.* **30** 7
[19] Moakher M, Shinbrot T and Muzzio F J 2000 Experimentally validated computations of flow, mixing and segregation of non-cohesive grains in 3d tumbling blenders *Powder Technol.* **109** 58–71
[20] Alexander A W, Shinbrot T and Muzzio F J 2001 Granular segregation in the double-cone blender: transitions and mechanisms *Phys. Fluids* **13** 578–87

[21] Alexander A, Muzzio F J and Shinbrot T 2003 Segregation patterns in v-blenders *Chem. Eng. Sci.* **58** 487–96
[22] Williams J C 1963 The segregation of powders and granular materials *Fuel Soc.* J **14** 29–34
[23] Gray J M N T and Thornton A R 2005 A theory for particle size segregation in shallow granular free-surface flows *Proc. Royal Soc. A* **461** 1447–73
[24] Marks B, Rognon P and Einav I 2012 Grainsize dynamics of polydisperse granular segregation down inclined planes *J. Fluid Mech.* **690** 499–511
[25] Ristow G H 1994 Particle mass segregation in a two-dimensional rotating drum *Europhys. Lett.* **28** 97
[26] Taberlet N, Losert W and Richard P 2004 Understanding the dynamics of segregation bands of simulated granular material in a rotating drum *Europhys. Lett.* **68** 522
[27] Muzzio F J, Shinbrot T and Glasser B J 2002 Powder technology in the pharmaceutical industry: the need to catch up fast *Powder Technology* **124** 1–7
[28] Massol-Chaudeur S, Berthiaux H and Dodds J A 2002 Experimental study of the mixing kinetics of binary pharmaceutical powder mixtures in a laboratory hoop mixer *Chemical Engineering Science* **57** 4053–65
[29] Naji L and Stannarius R 2009 Axial and radial segregation of granular mixtures in a rotating spherical container *Phys. Rev.* E **79** 031307
[30] Mohabuth N and Miles N 2005 The recovery of recyclable materials from waste electrical and electronic equipment (weee) by using vertical vibration separation *Resources, Conservation and Recycling* **45** 60–9
[31] Mohabuth N, Hall P and Miles N 2007 Investigating the use of vertical vibration to recover metal from electrical and electronic waste *Minerals Eng.* **20** 926–32
[32] Widmer R, Oswald-Krapf H, Sinha-Khetriwal D, Schnellmann M and Böni H 2005 Global perspectives on e-waste *Environ. Impact Assess. Rev.* **25** 436–58
[33] Sthiannopkao S and Wong M H 2013 Handling e-waste in developed and developing countries: Initiatives, practices, and consequences *Sci. Total Environ.* **463** 1147–53
[34] Nityanand N, Manley B and Henein H 1986 An analysis of radial segregation for different sized spherical solids in rotary cylinders *Metallurgical Transactions* B **17** 247–57
[35] Cantelaube F and Bideau D 1995 Radial segregation in a 2d drum: an experimental analysis *Europhys. Lett.* **30** 133
[36] Khakhar D V, McCarthy J J and Ottino J M 1997 Radial segregation of granular mixtures in rotating cylinders *Phys. Fluids* **9** 3600–14
[37] Jain N, Ottino J M and Lueptow R M 2005 Regimes of segregation and mixing in combined size and density granular systems: an experimental study *Granular Matter* **7** 69–81
[38] Hill K M, Jain N and Ottino J M 2001 Modes of granular segregation in a noncircular rotating cylinder *Phys. Rev.* E **64** 011302
[39] Rapaport D C 2002 Simulational studies of axial granular segregation in a rotating cylinder *Phys. Rev.* E **65** 061306
[40] Chen P, Ottino J M and Lueptow R M 2011 Granular axial band formation in rotating tumblers: a discrete element method study *New J. Phys.* **13** 055021
[41] Ottino J M and Khakhar D V 2000 Mixing and segregation of granular materials *Ann. Rev. Fluid Mech.* **32** 55–91
[42] McCarthy J J, Shinbrot T, Metcalfe G, Wolf J E and Ottino J M 1996 Mixing of granular materials in slowly rotated containers *AIChE J.* **42** 3351–63
[43] Meier S W, Cisar S E, Lueptow R M and Ottino J M 2006 Capturing patterns and symmetries in chaotic granular flow *Phys. Rev.* E **74** 031310
[44] Meier S W, Lueptow R M and Ottino J M 2007 A dynamical systems approach to mixing and segregation of granular materials in tumblers *Adv. In. Phys.* **56** 757–827
[45] Naji L and Stannarius R 2009 Axial and radial segregation of granular mixtures in a rotating spherical container *Phys. Rev.* E **79** 031307
[46] Christov I C, Ottino J M and Lueptow R M 2010 Chaotic mixing via streamline jumping in quasi-two-dimensional tumbled granular flows *Chaos: An Interdisciplinary Journal of Nonlinear Science* **20** 023102
[47] Prasad D V N and Khakhar D V 2010 Mixing of granular material in rotating cylinders with noncircular cross-sections *Phys. Fluids* **22** 103302
[48] Seiden G and Thomas P J 2011 Complexity, segregation, and pattern formation in rotating-drum flows *Rev. Mod. Phys.* **83** 1323–65
[49] Pohlman N A and Paprocki D F Jr 2012 Transient behavior of granular materials as result of tumbler shape and orientation effects *Granular Matter* **15** 1–9
[50] Zik O, Dov Levine S G, Lipson S, Shtrikman and Stavans J 1994 Rotationally induced segregation of granular materials *Phys. Rev. Lett.* **73** 644
[51] Cahn J W 1961 On spinodal decomposition *Acta Metallurgica* **9** 795–801
[52] Fan Y and Hill K M 2011 Theory for shear-induced segregation of dense granular mixtures *New J. Phys.* **13** 095009
[53] Fan Y and Hill K M 2011 Phase transitions in shear-induced segregation of granular materials *Phys. Rev. Lett.* **106** 218301
[54] Thornton A R, Gray J M N T and Hogg A J 2006 A three-phase mixture theory for particle size segregation in shallow granular free-surface flows *J. Fluid Mech.* **550** 1–26
[55] Middleton G V 1970 *Experimental Studies Related to Problems of Flysch Sedimentation* pp 253–72
[56] Savage S B and Lun C K K 1988 Particle size segregation in inclined chute flow of dry cohesionless granular solids *J. Fluid Mech.* **189** 311–35
[57] Savage S B 1993 *Mechanics of Granular Flows* (Vienna: Springer) pp 467–522
[58] Fan Y and Hill K M 2010 Shear-driven segregation of dense granular mixtures in a split-bottom cell *Phys. Rev.* E **81** 041303
[59] Aranson I S and Tsimring L S 2006 Patterns and collective behavior in granular media: theoretical concepts *Rev. Modern Phys.* **78** 641
[60] Harrington M, Weijs J H and Losert W 2013 Suppression and emergence of granular segregation under cyclic shear *Phys. Rev. Lett* **111** 078001
[61] Leighton D and Acrivos A 1987 The shear-induced migration of particles in concentrated suspensions *J. Fluid Mech.* **181** 415–39
[62] Hsiau S S and Hunt M L 1996 Granular thermal diffusion in flows of binary-sized mixtures *Acta mechanica* **114** 121–37
[63] Galvin J E, Dahl S R and Hrenya C M 2005 On the role of non-equipartition in the dynamics of rapidly flowing granular mixtures *J. Fluid Mech.* **528** 207–32
[64] Yoon D K and Jenkins J T 2006 The influence of different species granular temperatures on segregation in a binary mixture of dissipative grains *Physics of Fluids* **18** 073303
[65] Hill K M and Tan D S 2014 Segregation in dense sheared flows: gravity, temperature gradients, and stress partitioning *J. Fluid Mech.* **756** 54–88
[66] González S, Windows-Yule C R K, Luding S, Parker D J and Thornton A R 2015 Forced axial segregation in axially inhomogeneous rotating systems *Phys. Rev.* E **92** 022202

[67] Henein H, Brimacombe J K and Watkinson A P 1983 Experimental study of transverse bed motion in rotary kilns *Metall. Trans.* B **14** 191–205
[68] Davidson J, Scott D, Bird P, Herbert O, Powell A and Ramsay H 2000 Granular motion in a rotary kiln: the transition from avalanching to rolling *KONA Powder and Particle Journal* **18** 149–56
[69] Parker D J, Forster R N, Fowles P and Takhar P S 2002 Positron emission particle tracking using the new birmingham positron camera *Nuclear Instruments and Methods in Physics Research Section A: Accelerators, Spectrometers, Detectors and Associated Equipment* **477** 540–5
[70] Wildman R D, Huntley J M, Hansen J-P, Parker D J and Allen D A 2000 Single-particle motion in three-dimensional vibrofluidized granular beds *Phys. Rev.* E **62** 3826
[71] Parker D J, Broadbent C J, Fowles P, Hawkesworth M R and McNeil P 1993 Positron emission particle tracking-a technique for studying flow within engineering equipment *Nuclear Instruments and Methods in Physics Research Section A: Accelerators, Spectrometers, Detectors and Associated Equipment* **326** 592–607
[72] Choo K, Molteno T C A and Morris S W 1997 Traveling granular segregation patterns in a long drum mixer *Phys. Rev. Lett.* **79** 2975
[73] Wildman R D, Huntley J M and Parker D J 2001 Granular temperature profiles in three-dimensional vibrofluidized granular beds *Phys. Rev. E* **63** 061311
[74] Wildman R D, Huntley J M and Parker D J 2001 Convection in highly fluidized three-dimensional granular beds *Phys. Rev. Lett.* **86** 3304
[75] Windows-Yule C R K, Rivas N and Parker D J 2013 Thermal convection and temperature inhomogeneity in a vibrofluidized granular bed: The influence of sidewall dissipation *Phys. Rev. Lett.* **111** 038001
[76] Windows-Yule K and Parker D 2015 Density-driven segregation in binary and ternary granular systems *KONA Powder and Particle Journal* **32** 163–75
[77] Bridgewater J, Broadbent C J and Parker D J 1993 Study of the influence of blade speed on the performance of a powder mixer using positron emission particle tracking *Chemical Engineering Research & Design* **71** 675–81
[78] Parker D J, Dijkstra A E and Martin T W 1997 Positron emission particle tracking studies of spherical particle motion in rotating drums *Chem. Eng. Sci.* **52** 2011–22
[79] Fangary Y S, Barigou M, Seville JPK and Parker DJ 2000 Fluid trajectories in a stirred vessel of non-newtonian liquid using positron emission particle tracking *Chem. Eng. Sci.* **55** 5969–79
[80] Wildman R D and Parker D J 2002 Coexistence of two granular temperatures in binary vibrofluidized beds *Phys. Rev. Lett.* **88** 064301
[81] Yang S C 2006 Density effect on mixing and segregation processes in a vibrated binary granular mixture *Powder Technol.* **164** 65–74
[82] Hill K M and Kakalios J 1994 Reversible axial segregation of binary mixtures of granular materials *Phys. Rev.* E **49** R3610
[83] Hill K M and Kakalios J 1995 Reversible axial segregation of rotating granular media *Phys. Rev.* E **52** 4393
[84] Nakagawa M 1994 Axial segregation of granular flows in a horizontal rotating cylinder *Chem. Eng. Sci.* **49** 2540–4
[85] Finger T, Voigt A, Stadler J, Niessen H G, Naji L and Stannarius R 2006 Coarsening of axial segregation patterns of slurries in a horizontally rotating drum *Phys. Rev.* E **74** 031312
[86] Finger T, Schröter M and Stannarius R 2015 The mechanism of long-term coarsening of granular mixtures in rotating drums *New J. Phys.* **17** 093023
[87] Conway S L, Liu X and Glasser B J 2006 Instability-induced clustering and segregation in high-shear couette flows of model granular materials *Chem. Eng. Sci.* **61** 6404–23
[88] Chand R, Khaskheli M A, Qadir A, Ge B and Shi Q 2012 Discrete particle simulation of radial segregation in horizontally rotating drum: Effects of drum-length and non-rotating end-plates *Physica A* **391** 4590–6
[89] Dury C M, Ristow G H, Moss J L and Nakagawa M 1998 Boundary effects on the angle of repose in rotating cylinders *Phys. Rev.* E **57** 4491
[90] Lai P-Y, Jia L-C and Chan C K 1997 Friction induced segregation of a granular binary mixture in a rotating drum *Phys. Rev. Lett.* **79** 4994
[91] Newey M, Ozik J, Van der Meer S M, Ott E and Losert W 2004 Band-in-band segregation of multidisperse granular mixtures *Europhys. Lett.* **66** 205
[92] Sanfratello L and Fukushima E 2009 Experimental studies of density segregation in the 3d rotating cylinder and the absence of banding *Granular Matter* **11** 73–8
[93] Arntz M M H D, Beeftink H H, Otter den WK, Briels W J and Boom R M 2014 Segregation of granular particles by mass, radius, and density in a horizontal rotating drum *AIChE J.* **60** 50–9
[94] Kohav T, Richardson J T and Luss D 1995 Axial dispersion of solid particles in a continuous rotary kiln *AIChE J.* **41** 2465–75
[95] Nienow A W, Edwards M F and Harnby N 1997 *Mixing in the Process Industries* (Oxford: Butterworth-Heinemann)
[96] Ottino J M and Khakhar D V 2001 Fundamental research in heaping, mixing, and segregation of granular materials: challenges and perspectives *Powder Technology* **121** 117–22
[97] McClung D and Schaerer P A 2006 The avalanche handbook *The Mountaineers Books*
[98] Paul E L, Atiemo-Obeng V A and Kresta S M 2004 *Handbook of Industrial Mixing: Science and Practice* (New York: Wiley)